

RESEARCH ARTICLE

10.1002/2017GC006899

Utilizing ²¹⁰Po deficit to constrain particle dynamics in mesopelagic water, western South China Sea

Haoyang Ma¹, Weifeng Yang¹ , Lihao Zhang², Run Zhang¹, Min Chen¹ , Yusheng Qiu¹, and Minfang Zheng¹

¹State Key Laboratory of Marine Environmental Science and College of Ocean and Earth Sciences, Xiamen University, Xiamen, China, ²College of Environmental Science and Engineering, Guilin University of Technology, Guilin, China

Key Points:

- Large deficiencies of ²¹⁰Po were observed in mesopelagic water in the South China Sea
- Residence times and export fluxes of ²¹⁰Po indicate active particle cycling in mesopelagic water in the SCS
- The ²¹⁰Po-²¹⁰Pb pair was used to constrain the particle cycling in mesopelagic water

Correspondence to:

W. Yang,
wyang@xmu.edu.cn

Citation:

Ma, H., W. Yang, L. Zhang, R. Zhang, M. Chen, Y. Qiu, and M. Zheng (2017), Utilizing ²¹⁰Po deficit to constrain particle dynamics in mesopelagic water, western South China Sea, *Geochem. Geophys. Geosyst.*, 18, 1594–1607, doi:10.1002/2017GC006899.

Received 28 FEB 2017

Accepted 2 APR 2017

Accepted article online 12 APR 2017

Published online 18 APR 2017

Abstract The ²¹⁰Po-²¹⁰Pb pair is increasingly used as a proxy of quantifying organic carbon export from the euphotic zone. However, disequilibria between ²¹⁰Po and ²¹⁰Pb in mesopelagic water have been poorly studied. Here we present unusual deficiencies of ²¹⁰Po with respect to ²¹⁰Pb in mesopelagic water (200–1000 m) in the South China Sea (SCS). The total particulate matter (TPM) increased by up to 32% in the mesopelagic layer comparing with the euphotic zone. The total ²¹⁰Po/²¹⁰Pb ratio varied from 0.41 to 0.98 with an average of 0.72 ± 0.19, showing an enhanced removal of ²¹⁰Po in mesopelagic water. On average, particulate ²¹⁰Po and ²¹⁰Pb increased by 23% and 32% at the slope stations, respectively. These results indicated that the ²¹⁰Po deficits result from lateral transport, probably via benthic nepheloid layer. Based on the deficiency of ²¹⁰Po, the residence times of particulate ²¹⁰Po were estimated to range from 0.11 to 0.25 year (avg. 0.17 ± 0.07 year), allowing resuspended sediment to disperse over a long range. The export fluxes of ²¹⁰Po varied from 68 to 121 dpm m⁻² d⁻¹ with an average of 96 ± 27 dpm m⁻² d⁻¹, which was 6 times that out of the euphotic zone. Using the ²¹⁰Po deficits, the export fluxes of TPM out of the mesopelagic layer were quantified to vary from 4.19 to 10.20 g m⁻² d⁻¹, revealing a large amount of particles from the shelf to the SCS basin. This study suggests that ²¹⁰Po-²¹⁰Pb could be an effective tracer of tracking particle cycling in mesopelagic water.

1. Introduction

In seawater, ²¹⁰Po ($T_{1/2} = 138.4$ days) is mainly generated by its grandparent ²¹⁰Pb ($T_{1/2} = 22.3$ years) via radioactive decay. Both ²¹⁰Po and ²¹⁰Pb have very strong particle-reactive natures in seawater [Chuang et al., 2013; Yang et al., 2013]. In the euphotic zone, abundant biogenic particles usually introduce a quick sorption and sinking of ²¹⁰Po and ²¹⁰Pb on a short time scale, leading to insufficient time for ²¹⁰Po accumulation and resulting in an observable deficiency of ²¹⁰Po with respect to ²¹⁰Pb [Bacon et al., 1976; Nozaki and Tsunogai, 1976; Cochran et al., 1983]. Due to the tight link between particulate organic components and ²¹⁰Po or ²¹⁰Pb adsorption [Stewart et al., 2007; Yang et al., 2013, 2015a; Chuang et al., 2014; Rigaud et al., 2015], the disequilibria between ²¹⁰Po and ²¹⁰Pb have increasingly been used to trace the export flux of particulate organic carbon (POC) [Buesseler et al., 2008; Verdeny et al., 2009; Stewart et al., 2010; Roca-Martí et al., 2016; Su et al., 2017], biogenic silica [Friedrich and Rutgers van der Loeff, 2002], and nitrogen [Yang et al., 2011] out of the euphotic zone in the last decade. The ²¹⁰Po-²¹⁰Pb pair is also listed as one of the important proxies for investigating the oceanic particle dynamics in the ongoing GEOTRACES program [Church et al., 2012; Rigaud et al., 2013, 2015]. Since the half-life of ²¹⁰Po enables ²¹⁰Po-²¹⁰Pb pair to record information on particle cycling over time scales from days to seasons, this pair, together with sediment trap and ²³⁴Th-²³⁸U approach, is used to better decipher the POC export from the euphotic zone on different time scales [Hong et al., 2013; Ceballos-Romero et al., 2016; Maiti et al., 2016].

Although the application of ²¹⁰Po-²¹⁰Pb in the euphotic zone has been intensively studied recently, the cycling of ²¹⁰Po and its utilization in the mesopelagic (200–1000 m) and bathypelagic (1000–4000 m) zones are poorly understood to date [Kim, 2001; Hu et al., 2014]. It is generally accepted that ²¹⁰Po is in equilibrium with ²¹⁰Pb in deep water because the scarcity of particle allows ²¹⁰Po to reside longer and reach equilibrium as reported before, such as in North Atlantic [Bacon et al., 1976, 1988], Pacific [Turekian and Nozaki, 1980], and eastern and central Indian Ocean [Cochran et al., 1983]. However, the deficiencies of ²¹⁰Po with respect to ²¹⁰Pb have increasingly been found in mesopelagic water in the past years, e.g., in the Sargasso Sea

[Kim, 2001], Aleutian Basin [Hu *et al.*, 2014], the South China Sea (SCS) [Chung and Wu, 2005; Wei *et al.*, 2014, 2017], and at a few GEOTRACES stations in Atlantic Ocean [Church *et al.*, 2012; Rigaud *et al.*, 2015]. A few studies ascribe this deficiency to ^{210}Po uptake by bacterial [Kim, 2001; Chung and Wu, 2005], while some studies attribute it to the enhanced scavenging and removal of ^{210}Po in mesopelagic water introduced by laterally transported particulate matter [Hu *et al.*, 2014] and/or episodic settling of biological particulate [Wei *et al.*, 2014, 2017]. After analyzing the current progress in explaining ^{210}Po deficit in deep water, Rigaud *et al.* [2015] state that the deficiency of ^{210}Po in deep water is a major issue which may be addressed by GEOTRACES in the future. Although the reasons behind ^{210}Po deficit in deep water are still unclear, its preliminary application indicates that it could be an effective approach to investigate particle cycling in mesopelagic and bathypelagic water [Hu *et al.*, 2014].

In order to decipher the geochemical cycling of ^{210}Po and explore the application of ^{210}Po - ^{210}Pb to constrain particle dynamics in the mesopelagic zone, the deficiencies of ^{210}Po were examined in the western SCS. Recently, a few studies revealed the unusually higher particle fluxes in mesopelagic layer in the SCS [Liu *et al.*, 2014; Schroeder *et al.*, 2015], which probably result in a ^{210}Po deficit. Using the vertical variations of total particulate matter (TPM), particulate ^{210}Po and ^{210}Pb , combining published sediment trap data sets, the deficiency of ^{210}Po with respect to ^{210}Pb in mesopelagic water and its relation with shelf resuspended sediment were constrained in the western SCS. In addition, the deficit of ^{210}Po was used to quantify the residence time of particles and export fluxes of TPM out of the mesopelagic layer.

2. Materials and Methods

2.1. Study Site

The SCS is the largest marginal sea in the western tropical Pacific Ocean, including broad shelves in the north and west (Figure 1). The intraannual cycling of East Asian Monsoon results in the prevailing northeast winds from November to April and southwest winds from mid-May to mid-September in the SCS [Liu *et al.*, 2016]. The monsoon drives the surface current reversals [Shaw and Chao, 1994] and changes the mixing of surface and subsurface water [Li *et al.*, 2002], finally leading to a seasonal variation of POC export from the surface water [Cai *et al.*, 2015]. Together with the well-preserved sediment, the SCS is an ideal location for reconstructing paleoclimate in the East Asia [Wang *et al.*, 2014]. However, recent studies prove that the ubiquitous cross-shelf transport of particulate matter probably complicate the paleoenvironmental

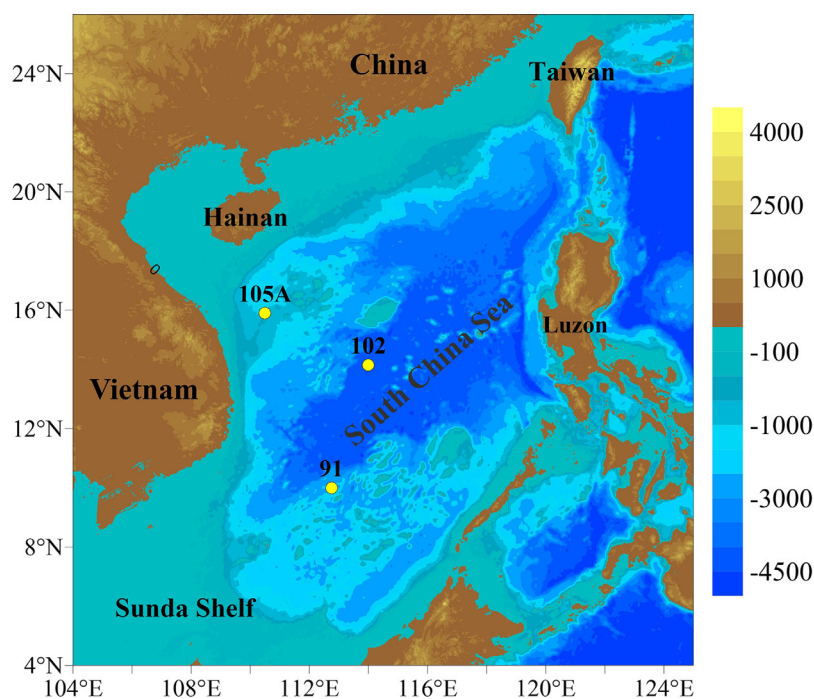


Figure 1. Sampling locations in the western South China Sea, 105A and 91 on the slope, and 102 in the basin.

information recorded in the SCS sediments [Gaye *et al.*, 2009; Liu *et al.*, 2014; Schroeder *et al.*, 2015; Dong *et al.*, 2016]. Thus, a well constraining of the particle cycling in mesopelagic and bathypelagic water would help us better understand the source-sink transport process of sediments in the SCS [Liu *et al.*, 2016].

2.2. Sampling and Analysis

Seawater samples were collected onboard *R/V Shiyang3* in August 2013. Sampling stations are mainly located in the western SCS (Figure 1), including two slope stations (105A and 91) and a basin station (102). Station 105A is close to the shelf and shows a depth of 775 m. Station 91 has a water depth of 1756 m, close to the SCS basin. Station 102 is near the central basin with a depth of 4302 m. Seawater was sampled using a CTD-rossette system. At each depth, 10 L of seawater was collected, and immediately filtered through a pre-weighed polycarbonate filter membrane with 0.4 μm pore size for collecting TPM.

The filtrate was acidified using hydrochloric acid to a pH value less than 2.0, and predetermined amount of ^{209}Po , Pb^{2+} spikes, and Fe^{3+} carrier were added. After 24 h, ammonium hydroxide was added to form $\text{Fe}(\text{OH})_3$ precipitate and adsorb Po and Pb isotopes (i.e., ^{209}Po , ^{210}Po , ^{210}Pb , and stable Pb) [Church *et al.*, 2012; Rigaud *et al.*, 2013]. The precipitate was settled overnight, and collected via centrifugation. Then, the precipitate was redissolved in a 0.5 M HCl solution. Ascorbic acid, hydroxylamine hydrochloride, and sodium citrate were added to chelate Fe^{3+} and eliminate the influence of other ions during Po plating. Po isotopes including ^{209}Po and ^{210}Po were plated on a silver disc at 90°C for 4 h under stirring with a Teflon-coated stirring bar [Yang *et al.*, 2013, 2015a]. Particulate samples were dried at 60°C to constant weights in order to estimate the TPM contents. Then, ^{209}Po and Pb^{2+} yield tracers were added and digested using mixed acids (HClO_4 , HNO_3 , and HF). The autodeposition of Po isotopes on the Ag disc was the same to that of dissolved samples. The activities of ^{209}Po and ^{210}Po were counted by an Alpha Analyst System (ORTEC). The recoveries of ^{210}Po were determined by initially added and finally counted ^{209}Po . ^{210}Pb was measured via ^{210}Po after 2 years. The yields of ^{210}Pb were determined through the added stable Pb and measured Pb using an atomic absorption spectrometry. Activity concentrations of ^{210}Po and ^{210}Pb were decay corrected back to the sampling time, and detector background and reagent blank were also corrected.

3. Results

3.1. Hydrologic Parameters

Surface water showed significant differences in both temperature and salinity between the three stations (Figure 2). The mixed layer ($\Delta T = 0.8^\circ\text{C}$) [Kara *et al.*, 2000] depths (i.e., MLD) were 35, 70, and 48 m for 105A, 91, and 102, respectively. The differences in the means of temperature and salinity in the mixed layer reached 0.89°C and 1.038, corresponding to a large heterogeneity of surface water. However, temperature and salinity were comparable to each other in mesopelagic water (e.g., 200–700 m). For instance, salinity, on average, was 34.450 ± 0.050 , 34.466 ± 0.043 , and 34.453 ± 0.050 at 105A, 91, and 102, respectively. It is obvious that the mesopelagic waters at the three studied sites have similar characteristics. Such a phenomenon is consistent with the anticyclonic current between 150 and 900 m in August in the SCS [Chao *et al.*, 1996], which could transport mesopelagic water from station 91 to 102.

3.2. ^{210}Po and ^{210}Pb Activity Concentrations

The activity concentrations of dissolved ^{210}Po ($^{210}\text{Po}_D$) ranged from 2.02 ± 0.30 to 8.64 ± 0.87 dpm 100 L^{-1} (Table 1), comparable to the values of 1.78 ± 0.25 to 9.60 ± 0.85 dpm 100 L^{-1} between 0 and 1000 m at the SouthEast Asian Time-series Study (SEATS) station in the SCS [Wei *et al.*, 2014]. Dissolved ^{210}Pb ($^{210}\text{Pb}_D$) varied from 1.07 ± 0.42 to 10.70 ± 1.14 dpm 100 L^{-1} (avg. 6.38 ± 1.53 dpm 100 L^{-1}), which also coincided with those of 2.55 ± 0.16 to 11.80 ± 0.65 dpm 100 L^{-1} (avg. 7.55 ± 1.83 dpm 100 L^{-1}) at SEATS [Wei *et al.*, 2014]. Particulate ^{210}Po ($^{210}\text{Po}_P$) and ^{210}Pb ($^{210}\text{Pb}_P$) averaged 0.90 ± 0.61 and 1.47 ± 1.03 dpm 100 L^{-1} , respectively (Figure 2). $^{210}\text{Pb}_P$ in the SCS was much higher than open oceans, such as the northern Atlantic Ocean (avg. 0.76 ± 0.95 dpm 100 L^{-1}) [Rigaud *et al.*, 2015]. On average, both dissolved ^{210}Po and ^{210}Pb accounted for the majority (85% and 82%) of the total ^{210}Po and ^{210}Pb , showing a typical characteristic of open seawater. The total ^{210}Po ($^{210}\text{Po}_T$) and ^{210}Pb ($^{210}\text{Pb}_T$) varied from 2.59 ± 0.34 to 9.64 ± 1.03 dpm 100 L^{-1} and from 3.71 ± 0.46 to 13.22 ± 1.06 dpm 100 L^{-1} with the averages of 5.87 ± 1.69 and 8.15 ± 2.36 dpm 100 L^{-1} . These results were comparable to $^{210}\text{Po}_T$ and $^{210}\text{Pb}_T$ at SEATS (avg. 5.89 ± 2.11 and 8.53 ± 1.88 dpm 100 L^{-1}) [Wei *et al.*, 2014].

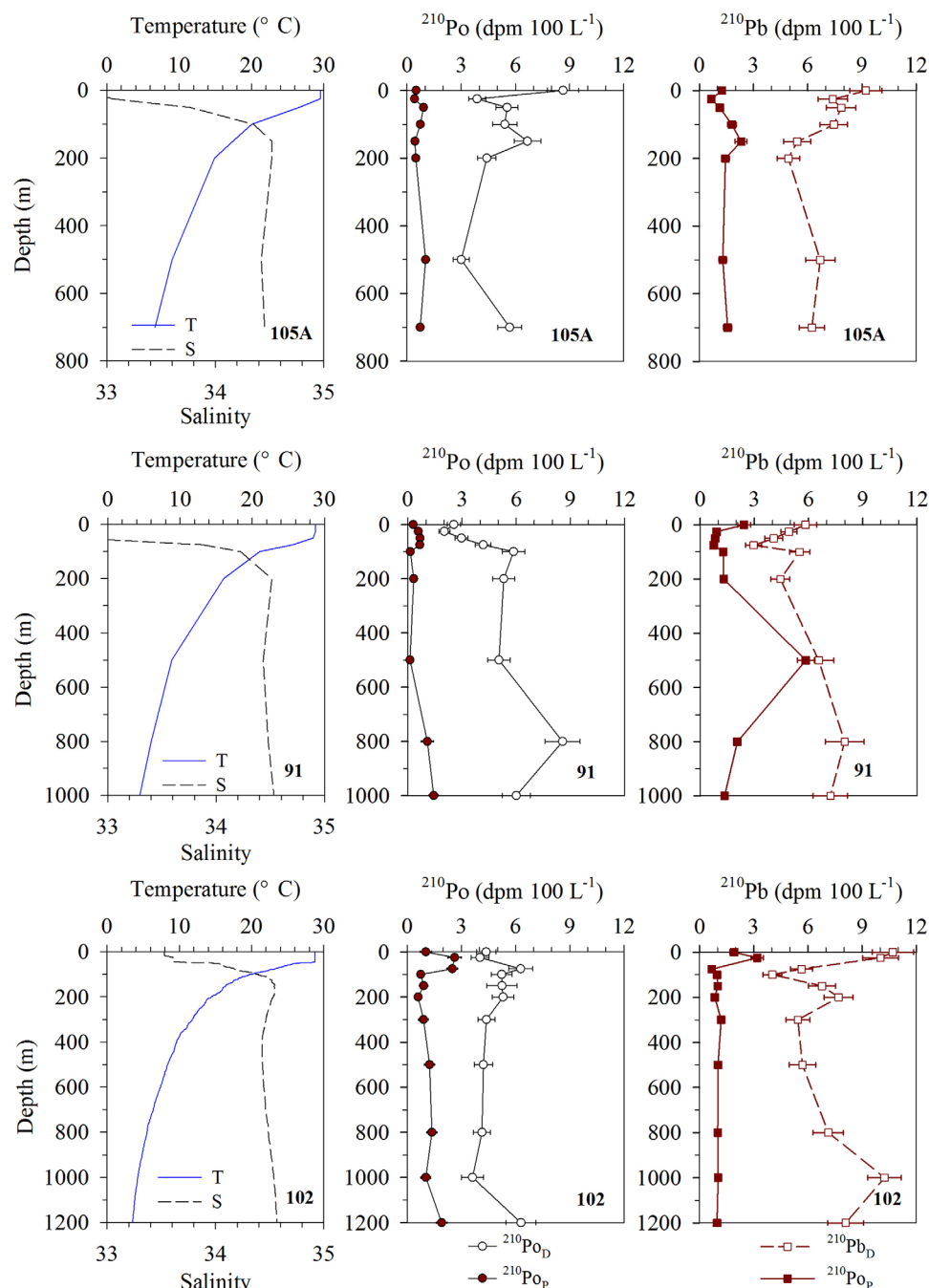


Figure 2. Profiles of temperature, salinity, dissolved ^{210}Po and ^{210}Pb , particulate ^{210}Po and ^{210}Pb in the western South China Sea.

In the euphotic zone (0–100 m), $^{210}\text{Pb}_D$ and $^{210}\text{Pb}_T$ showed the highest activity concentrations in surface water at all stations (Figure 2), corresponding to its dominant atmospheric source. Overall, $^{210}\text{Po}_T$ was in deficit with respect to $^{210}\text{Pb}_T$ in the mixed layer (Figure 3), as reported in the SCS [Yang *et al.*, 2006; Wei *et al.*, 2014]. However, $^{210}\text{Po}_T$ showed higher values than $^{210}\text{Pb}_T$ (i.e., excess ^{210}Po) below the mixed layer at stations 91 and 102, ascribing to the remineralization of particulate organic matter [Bacon *et al.*, 1976; Yang *et al.*, 2009]. Notably, $^{210}\text{Po}_T$ showed evident deficiencies relative to its parent nuclide ^{210}Pb in mesopelagic water (i.e., 200–1000 m) at all studied stations though there were differences in the deficient extent (Figure 3). In fact, similar deficiency occurred at the SEATS station in the northern SCS [Wei *et al.*, 2014]. This deficiency provided a contrast to the equilibrium status between $^{210}\text{Po}_T$ and $^{210}\text{Pb}_T$ below the remineralization

Table 1. Temperature, Salinity, TPM Concentrations, and Activity Concentrations of Dissolved and Particulate ^{210}Po and ^{210}Pb in the Western South China Sea

Stn.	Depth (m)	T (°C)	S	TPM (mg L ⁻¹)	$^{210}\text{Po}_D$	$^{210}\text{Po}_P$	$^{210}\text{Po}_T$	$^{210}\text{Pb}_D$	$^{210}\text{Pb}_P$	$^{210}\text{Pb}_T$
					(dpm 100 L ⁻¹)					
105A	0	29.51	32.80	0.27 ± 0.01	8.64 ± 0.87	0.50 ± 0.12	9.14 ± 0.88	9.21 ± 0.89	1.25 ± 0.18	10.46 ± 0.91
	25	29.54	33.05	0.41 ± 0.01	3.88 ± 0.47	0.42 ± 0.12	4.29 ± 0.48	7.39 ± 0.82	0.66 ± 0.10	8.04 ± 0.82
	50	26.63	33.76	0.43 ± 0.01	5.53 ± 0.62	0.91 ± 0.16	6.45 ± 0.64	7.85 ± 0.82	1.14 ± 0.16	8.99 ± 0.83
	100	20.04	34.35	0.33 ± 0.01	5.41 ± 0.68	0.73 ± 0.20	6.14 ± 0.71	7.44 ± 0.76	1.81 ± 0.24	9.25 ± 0.79
	150	17.44	34.52	0.36 ± 0.01	6.67 ± 0.75	0.44 ± 0.13	7.11 ± 0.76	5.42 ± 0.75	2.32 ± 0.33	7.74 ± 0.82
	200	14.89	34.52	0.08 ± 0.01	4.41 ± 0.50	0.49 ± 0.14	4.90 ± 0.52	4.93 ± 0.62	1.44 ± 0.21	6.38 ± 0.66
91	500	9.02	34.42	0.65 ± 0.01	3.00 ± 0.44	1.03 ± 0.22	4.02 ± 0.50	6.69 ± 0.81	1.30 ± 0.21	7.99 ± 0.84
	700	6.67	34.45	0.75 ± 0.01	5.68 ± 0.66	0.72 ± 0.22	6.40 ± 0.70	6.23 ± 0.69	1.56 ± 0.22	7.79 ± 0.73
	0	28.73	32.36	0.31 ± 0.01	2.54 ± 0.37	0.30 ± 0.10	2.83 ± 0.38	5.83 ± 0.62	2.43 ± 0.36	8.26 ± 0.72
	25	28.75	32.39	0.69 ± 0.01	2.02 ± 0.30	0.57 ± 0.15	2.59 ± 0.34	4.92 ± 0.45	0.90 ± 0.12	5.82 ± 0.46
	50	28.41	32.72	0.43 ± 0.01	2.97 ± 0.35	0.68 ± 0.15	3.64 ± 0.38	4.08 ± 0.49	0.83 ± 0.11	4.91 ± 0.50
	75	25.59	33.88	0.47 ± 0.01	4.17 ± 0.43	0.66 ± 0.14	4.83 ± 0.45	2.96 ± 0.45	0.75 ± 0.11	3.71 ± 0.46
	100	21.03	34.22	0.76 ± 0.01	5.85 ± 0.62	0.13 ± 0.05	5.98 ± 0.62	5.51 ± 0.57	1.27 ± 0.16	6.78 ± 0.59
	200	16.03	34.51	0.68 ± 0.01	5.30 ± 0.61	0.32 ± 0.12	5.62 ± 0.62	4.44 ± 0.52	1.31 ± 0.14	5.75 ± 0.54
	500	8.87	34.43	0.56 ± 0.01	5.04 ± 0.62	0.12 ± 0.05	5.16 ± 0.62	6.56 ± 0.84	5.85 ± 0.47	12.41 ± 0.96
	800	6.00	34.48	0.37 ± 0.01	8.57 ± 0.97	1.08 ± 0.33	9.64 ± 1.03	8.00 ± 1.08	2.06 ± 0.20	10.06 ± 1.10
102	1000	4.42	34.53	0.56 ± 0.01	6.00 ± 0.78	1.43 ± 0.27	7.42 ± 0.82	7.21 ± 0.95	1.35 ± 0.14	8.56 ± 0.96
	0	28.74	33.53	0.53 ± 0.01	4.37 ± 0.54	1.03 ± 0.31	5.40 ± 0.62	10.70 ± 1.14	1.91 ± 0.22	12.62 ± 1.16
	25	28.70	33.46	0.57 ± 0.01	4.03 ± 0.50	2.62 ± 0.37	6.65 ± 0.62	10.02 ± 1.00	3.20 ± 0.34	13.22 ± 1.06
	50	26.18	33.98	0.58 ± 0.01	5.28 ± 0.53	0.79 ± 0.17	6.07 ± 0.56	n.d. ^a	n.d.	n.d.
	75	22.93	34.15	1.05 ± 0.01	6.29 ± 0.68	2.49 ± 0.29	8.78 ± 0.73	5.65 ± 0.60	0.68 ± 0.10	6.33 ± 0.61
	100	19.38	34.39	0.56 ± 0.01	5.23 ± 0.57	0.75 ± 0.11	5.98 ± 0.58	4.03 ± 0.52	0.97 ± 0.13	5.00 ± 0.54
	150	16.44	34.53	0.48 ± 0.01	5.24 ± 0.83	0.91 ± 0.23	6.15 ± 0.86	6.79 ± 0.75	1.01 ± 0.13	7.80 ± 0.76
	200	14.53	34.52	0.33 ± 0.01	5.31 ± 0.59	0.60 ± 0.16	5.91 ± 0.62	7.70 ± 0.79	0.85 ± 0.11	8.55 ± 0.80
	300	11.77	34.46	0.38 ± 0.01	4.39 ± 0.48	0.90 ± 0.26	5.29 ± 0.55	5.45 ± 0.66	1.20 ± 0.17	6.65 ± 0.68
	500	8.44	34.43	0.39 ± 0.01	4.21 ± 0.50	1.23 ± 0.28	5.45 ± 0.57	5.70 ± 0.73	1.03 ± 0.16	6.73 ± 0.75
	800	5.52	34.48	0.51 ± 0.01	4.14 ± 0.47	1.36 ± 0.27	5.51 ± 0.54	7.13 ± 0.84	1.01 ± 0.14	8.14 ± 0.85
	1000	4.34	34.53	0.37 ± 0.01	3.61 ± 0.61	1.03 ± 0.27	4.65 ± 0.66	10.25 ± 0.93	1.03 ± 0.15	11.27 ± 0.94
1200	3.57	34.56	0.44 ± 0.01	6.30 ± 0.82	1.91 ± 0.29	8.21 ± 0.87	8.09 ± 1.00	0.97 ± 0.14	9.07 ± 1.01	

^an.d. denotes not data.

layer in general mesopelagic water [Bacon *et al.*, 1976; Roca-Martí *et al.*, 2016]. At the same time, the average activity concentration of $^{210}\text{Po}_P$ increased from 0.69 ± 0.08 dpm 100 L⁻¹ in the euphotic zone to 0.85 ± 0.11 dpm 100 L⁻¹ in the mesopelagic layer at station 105A, and from 0.53 ± 0.06 to 0.65 ± 0.11 dpm 100 L⁻¹ at station 91. On average, the $^{210}\text{Pb}_P$ activities increased from 1.20 ± 0.09 to 1.58 ± 0.12 dpm 100 L⁻¹ and from 1.08 ± 0.09 to 3.41 ± 0.14 dpm 100 L⁻¹ (Figure 4). The concurrently occurrences of ^{210}Po deficit and elevated $^{210}\text{Po}_P$ and $^{210}\text{Pb}_P$ activities corresponded to an enhanced removal of ^{210}Po below the remineralization layer in the western SCS.

3.3. TPM

For all samples, the TPM contents ranged from 0.08 to 1.05 mg L⁻¹ with an averaging of 0.48 ± 0.01 mg L⁻¹ (Table 1), showing the typical characteristic of open seawater. Notably, TPM did not show a decrease from surface downward to mesopelagic water at the two slope stations (i.e., 105A and 91) (Figure 3). At station 105A, TPM averaged 0.38 ± 0.01 mg L⁻¹ in the upper 100 m, and it increased to 0.50 ± 0.01 mg L⁻¹ in the 200–700 m layer (Figure 4), corresponding to an addition of TPM in mesopelagic water. At station 91, TPM showed comparable contents of 0.52 mg L⁻¹ in euphotic and mesopelagic water on average. At the basin station 102, TPM varied from 0.53 to 1.05 mg L⁻¹ with an average of 0.65 ± 0.01 mg L⁻¹ in the euphotic zone. However, a decrease of the TPM content was observed in mesopelagic water (200–1000 m), ranging from 0.33 to 0.51 mg L⁻¹ and averaging 0.40 ± 0.01 mg L⁻¹.

4. Discussion

4.1. ^{210}Po Deficiency in Mesopelagic Water

In the euphotic zone, ^{210}Po is usually deficient with respect to ^{210}Pb due to their rapid removal induced by plenty of biogenic particles [Nozaki *et al.*, 1998; Stewart *et al.*, 2010]. Below the euphotic zone, ^{210}Po quickly reaches an equilibrium status with ^{210}Pb (i.e., ^{210}Po equals to ^{210}Pb) [Murray *et al.*, 2005; Roca-Martí *et al.*, 2016].

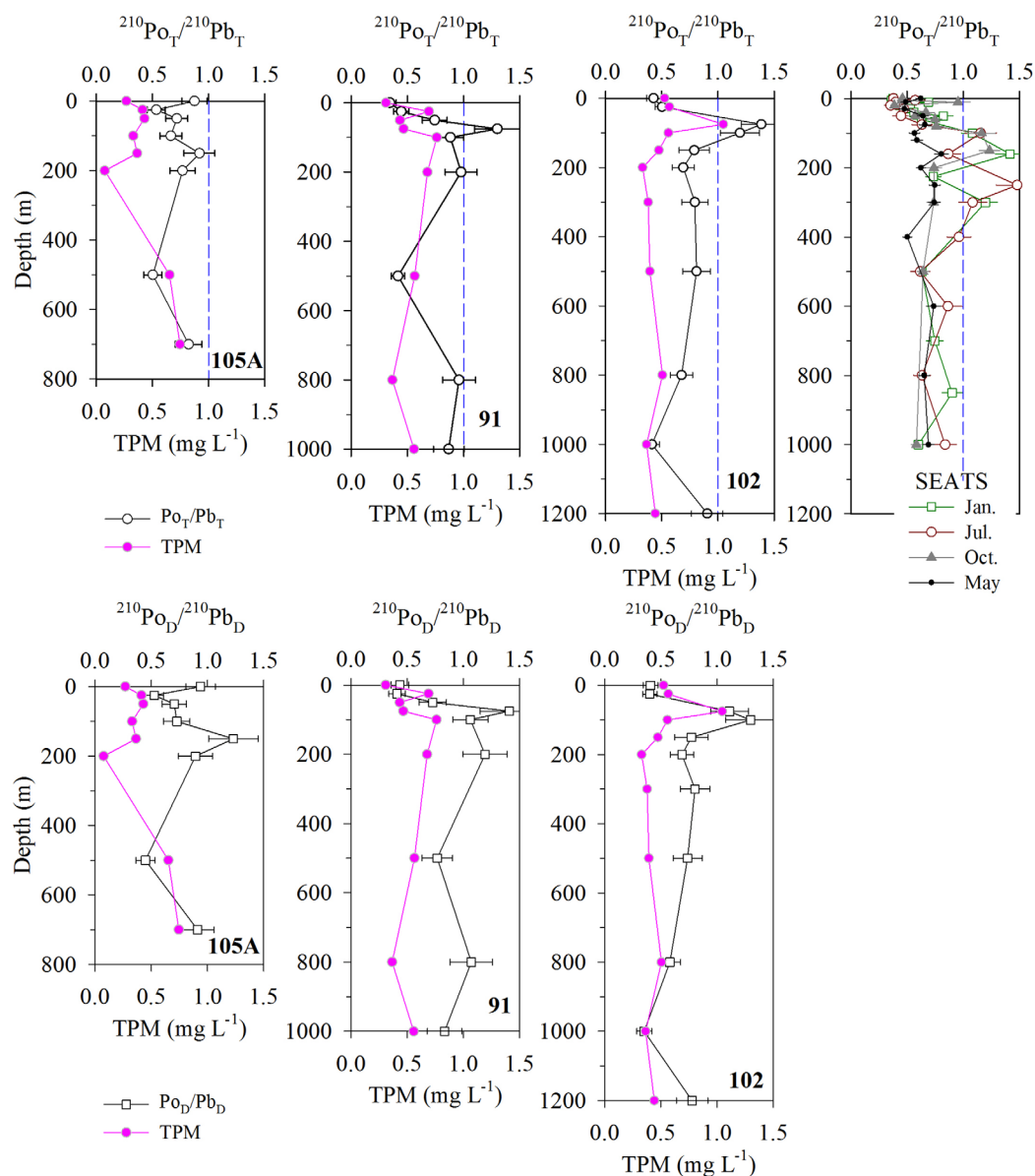


Figure 3. Profiles of the activity ratios of ^{210}Po to ^{210}Pb in dissolved and total fractions in the South China Sea (105A, 91, and 102 in this study) and at the SEATS station (data from Wei et al. [2014]).

Sometimes, ^{210}Po activity concentrations are higher than ^{210}Pb at the bottom of the euphotic zone or in the upper mesopelagic zone as a result of ^{210}Po release from sinking particles during particle remineralization (Figure 3) [Bacon et al., 1976; Cochran et al., 1983; Yang et al., 2009]. In most mesopelagic and bathypelagic water, ^{210}Po is usually in equilibrium with ^{210}Pb [Bacon et al., 1976; Nozaki and Tsunogai, 1976; Cochran et al., 1983], owing to its longer residence time (>2 years) compared to its half-life. However, the profiles of the $^{210}\text{Po}_T/^{210}\text{Pb}_T$ ratio in the present study showed an evident ^{210}Po deficit in mesopelagic water (Figure 3). This ratio varied from 0.41 to 0.98 with an average of 0.72 ± 0.19 , which was only slightly higher than the average of 0.58 ± 0.17 (from 0.34 to 0.87) in the euphotic zone at the three stations (*t* test, $p < 0.05$). A recent study also identified similar deficiency of ^{210}Po in mesopelagic water in the northern SCS [Wei et al., 2014]. Such deficiencies in the total ^{210}Po implied an enhanced removal of ^{210}Po over a short time scale in mesopelagic water in the western SCS. The distributions of $^{210}\text{Po}_D/^{210}\text{Pb}_D$ also revealed the enhanced scavenging of ^{210}Po in mesopelagic water (Figure 3). Overall, the TPM distributions mirror the distributions of $^{210}\text{Po}_D/^{210}\text{Pb}_D$, indicating more adsorption of ^{210}Po induced by the elevation of TPM in

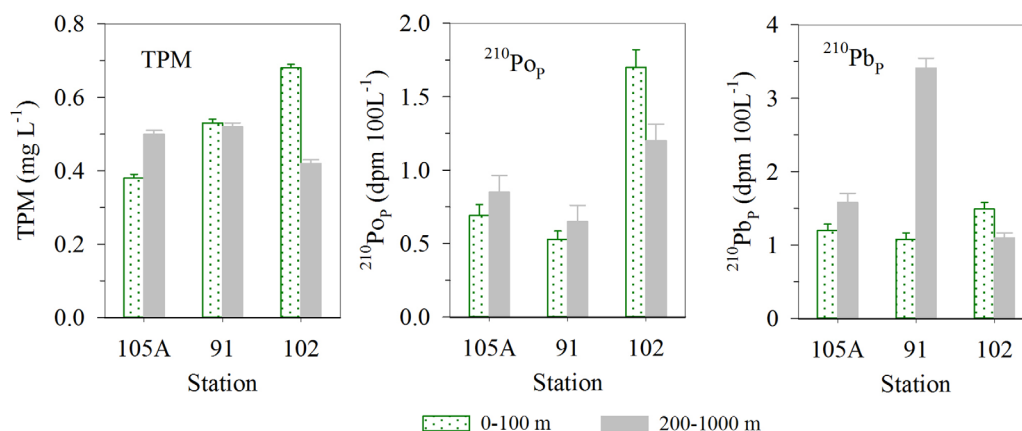


Figure 4. Comparisons of depth-weighted TPM concentration, activity concentrations of ^{210}Po and ^{210}Pb between mesopelagic water (200–1000 m) and euphotic water (0–100 m).

the mesopelagic layer. In general, the predominant removal of ^{210}Po is sinking after being adsorbed onto particulate matter [Yang *et al.*, 2013; Rigaud *et al.*, 2015; Wei *et al.*, 2017] in a manner similar to the particle-reactive thorium isotopes [Yang *et al.*, 2016]. Since ^{210}Po reached equilibrium with ^{210}Pb at the top mesopelagic layer for all stations (Figure 3), the deficits of ^{210}Po in mesopelagic water could not result from the sinking particles out of the euphotic zone. Instead, some other original particles, such as lateral transport of shelf resuspended sediment, would interpret this scenario. A study in the Aleutian Basin observed ^{210}Po deficits in mesopelagic and bathypelagic water, and attested to the causal link between the shelf-derived particle and ^{210}Po deficiency [Hu *et al.*, 2014]. Two available case studies identified the benthic nepheloid layers in the SCS based on multiple proxies of ^{210}Pb , turbidity, and particle grain size [Chung *et al.*, 2004; Zhang *et al.*, 2014]. Together with the wide increased particle flux measured in mesopelagic water comparing with the euphotic zone [Lahajnar *et al.*, 2007; Gaye *et al.*, 2009; Liu *et al.*, 2014], we hypothesize that the unusually deficiency of ^{210}Po in the mesopelagic layer is from its scavenging and removal by lateral transported particulate matter, probably via benthic nepheloid layer.

Indeed, the elevations of TPM and $^{210}\text{Pb}_p$ activity concentration support this hypothesis. As shown in Figure 4, the averaged TPM content at station 105A increased about 32%, from $0.38 \pm 0.01 \text{ mg L}^{-1}$ in the euphotic zone to $0.50 \pm 0.01 \text{ mg L}^{-1}$ in the mesopelagic layer. This difference between the euphotic and mesopelagic layers was much larger than the uncertainties. At station 91 with a deeper seafloor than 105A, the TPM contents showed the same value in euphotic and mesopelagic water, averaging $0.52 \pm 0.01 \text{ mg L}^{-1}$ (Table 1). It has been revealed that particulate matter in the euphotic zone is rich in biogenic components (i.e., organic matter and biogenic silica) in the western SCS [Wei *et al.*, 2011; Cai *et al.*, 2015; Yang *et al.*, 2015b]. During settling below the euphotic zone, organic components degrade up to >50% in the SCS [Chen *et al.*, 1998; Yang *et al.*, 2009]; the TPM contents would decrease in the mesopelagic layer if there were no additional inputs of particulate matter. Thus, the increase of TPM in mesopelagic water over the slope indicated some particle sources other than sinking from the euphotic zone. At the same time, particulate ^{210}Po and ^{210}Pb also showed increases to a varying degree in the mesopelagic layer at the slope stations 105A and 91 (Figure 4). For example, $^{210}\text{Po}_p$ activity concentrations increased by 23% and 32% in mesopelagic water comparing with the euphotic zone, respectively. $^{210}\text{Pb}_p$ also increased by more than 23% on average (Table 1). The $^{210}\text{Po}_p$ and $^{210}\text{Pb}_p$ elevations were much larger than their uncertainties (<14% averagely), lending support to these increases. At the basin station 102, the elevations of TPM and $^{210}\text{Po}_p$ were not observed in mesopelagic water (Figure 4); however, the $^{210}\text{Po}_T$ deficit with respect to $^{210}\text{Po}_T$ implied enhanced removal of ^{210}Po within this regime (Figure 3), probably owing to the descending of laterally transported particulate matter in the basin region.

Interestingly, the penetrating depth of ^{210}Po deficit in mesopelagic water seems to get deeper from the shallowest slope station 105A to the basin station 102 (Figure 3). ^{210}Po deficiency occurred between 200 and 700 m at 105A, below 700 m ^{210}Po was nearly in equilibrium with ^{210}Pb . At station 91, ^{210}Po deficiency reached a depth close to 800 m. At station 102, ^{210}Po deficiency extended down to >1000 m. In the

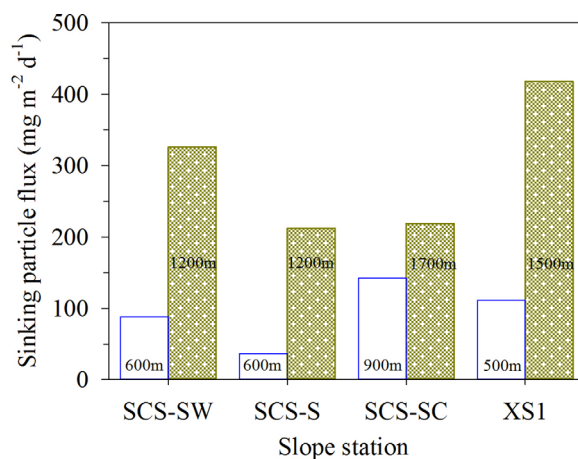


Figure 5. Particle fluxes at different depths over the slope in the SCS to illustrate the higher particle fluxes out of the lower mesopelagic layer compared with the upper mesopelagic layer. The numbers (i.e., 600, 700, and 1200 m) represent the depths determining flux. Data at SCS-SW, SCS-S, and SCS-SC are from *Lahajnar et al.* [2007] and *Gaye et al.* [2009], and data at XS1 are from *Liu et al.* [2014], which were measured using the sediment traps.

(Figure 5) [*Lahajnar et al.*, 2007; *Gaye et al.*, 2009; *Liu et al.*, 2014; *Schroeder et al.*, 2015]. Based on these studies, it seems that the transport of shelf sediment to the basin is ubiquitous in the SCS. Multiple proxies, including minerals, rare earth elements, neodymium and strontium isotopes, and amino acids and hexosamines, actually provide evidence for the cross-shelf transport of resuspended sediment in the entire SCS [*Liu et al.*, 2013, 2014; *Schroeder et al.*, 2015; *Liu et al.*, 2016]. Although the dynamics of cross-shelf transport in mesopelagic water is poorly understood, the stable deep current with an average velocity of 5–6 cm s⁻¹ is expected to be responsible for the lateral particle transport in the SCS [*Liu et al.*, 2014, 2016].

Since the lateral transport of particulate matter introduced the deficit of ²¹⁰Po in mesopelagic water in the western SCS (Figure 3), the disequilibrium between ²¹⁰Po and ²¹⁰Pb could enable us to constrain the particle dynamics, such as particle flux and resident time scale of particle in the mesopelagic layer.

4.2. Resident Time Scale and Removal of ²¹⁰Po in Mesopelagic Water

Based on the mass balance of ²¹⁰Po in the mesopelagic layer, the variability in the inventories of dissolved and particulate ²¹⁰Po can be expressed as

$$\frac{dI_{PoD}}{dt} = \lambda_{Po}(I_{PbD} - I_{PoD}) - kI_{PoD} \quad (1)$$

$$\frac{dI_{PoP}}{dt} = \lambda_{Po}(I_{PbP} - I_{PoP}) + kI_{PoD} - \phi I_{PoP} \quad (2)$$

where I_{PoD} and I_{PbD} represent the inventories of dissolved ²¹⁰Po and ²¹⁰Pb (in dpm m⁻²); I_{PoP} and I_{PbP} represent the inventories of particulate ²¹⁰Po and ²¹⁰Pb (in dpm m⁻²); k and ϕ are the scavenging (from dissolved to particulate phase) and removal (sinking out of the specific water regime) constants of ²¹⁰Po in the unit of day⁻¹; and λ_{Po} is the decay constant of ²¹⁰Po (0.0050 day⁻¹). Thus, kI_{PoD} and ϕI_{PoP} represent the scavenging flux (J) and removal flux (P) of ²¹⁰Po in the unit of dpm m⁻² d⁻¹. This model was also applied to the euphotic zone after adding the atmospheric deposition flux of ²¹⁰Po in equation (1). Usually, atmospheric flux of ²¹⁰Po is neglected due to its minor contribution to the bulk ²¹⁰Po in surface water [*Bacon et al.*, 1976; *Yang et al.*, 2006, 2009]. However, the atmospheric flux of ²¹⁰Po in the SCS is estimated to be 1.64 dpm m⁻² d⁻¹ [*Wei et al.*, 2011], accounting for about 18% of the total ²¹⁰Po source. Hence, this term was included in this study. The inventories of ²¹⁰Po and ²¹⁰Pb were calculated using the trapezoidal integral:

$$I = \int_{z=top}^{z=bottom} A dz \tag{3}$$

where $z = top$ represents the depths of the top euphotic zone and mesopelagic layer (i.e., 0 and 200 m in this study), $z = bottom$ represents the depths of euphotic and mesopelagic zone bottom (i.e., 100 and 1000 m), and A is the activity concentration of ^{210}Po or ^{210}Pb in dissolved and particulate phases. Based on the comparison between the steady state and nonsteady state results of the mass balance model of ^{210}Po in the SCS, *Wei et al.* [2014] find that there is no difference when the errors are taken into account. Thus, equations (1) and (2) were solved in the steady state. The residence times of dissolved and particulate ^{210}Po were estimated from the reciprocals of the scavenging and removal constants (Table 2).

The residence times of particulate ^{210}Po at the slope stations (i.e., 105A and 91) ranged from 0.11 to 0.16 year within the mesopelagic layer (averaging 0.13 ± 0.04 year), comparable to the residence times of TPM in a hydrothermal plume over the Southwest Indian Ridge [*Yang et al.*, 2016]. Such a time scale allows particulate matter to move over a very long range as proved in general deep water [*Siegel et al.*, 2008] and in the mesopelagic or bathypelagic hydrothermal plumes [*Wang et al.*, 2012; *Estapa et al.*, 2015]. Thus, the residence times of particulate ^{210}Po provide supports for the transport of resuspended shelf sediment into the SCS basin. At the basin station 102, the residence time of particulate ^{210}Po was 0.25 year, about twofold of those observed on the slope (Table 2). Based on the data sets of ^{210}Po and ^{210}Pb collected at the SEATS station [*Wei et al.*, 2014], the residence times of particulate ^{210}Po varied from 0.18 to 0.75 year. Together with our results, TPM appeared to reside for a longer time in mesopelagic water in the SCS basin than those on the slope. Given dissolved ^{210}Po , its residence times, in most cases, were less than 1.5 years in mesopelagic water (Table 2). Consequently, the residence times of the bulk ^{210}Po regime mainly fall in a range of 1–2 years.

Although there have been few studies on the resident times of ^{210}Po in mesopelagic and bathypelagic water [*Bacon et al.*, 1976; *Kadko et al.*, 1987; *Hu et al.*, 2014], they provide an opportunity for us to look into the scavenging and removal intensity of ^{210}Po in various deep water. As unique settings, ^{210}Po in the hydrothermal plumes close to the vents, characterized by Mn-/Fe-enriched particles, have residence times of about 1 year [*Kadko et al.*, 1987], corresponding to quick scavenging and removal of ^{210}Po in these systems. In hydrothermal plumes far from the vents, ^{210}Po shows much longer residence time [*Rigaud et al.*, 2015], probably due to the weakened influence of hydrothermal particles. In general deep waters, ^{210}Po usually resides for several years which enable it to reach equilibrium with ^{210}Pb [*Bacon et al.*, 1976]. In deep water receiving cross-shelf transported particle, the residence times of ^{210}Po varied from 0.9 to 1.9 years [*Hu et al.*, 2014], falling in the range of one to several years. Obviously, the residence times of ^{210}Po in mesopelagic water in the SCS (Table 2) were shorter than general deep water, and longer than the typical hydrothermal plumes. Such a scenario indicated that the scavenging of ^{210}Po in mesopelagic water in the SCS is stronger comparing with general deep water; however, this process is weaker than those observed in hydrothermal

Table 2. Scavenging (k) and Removal Constants (φ) of ^{210}Po , Residence Times of Dissolved (τ_{PoD}) and Particulate ^{210}Po (τ_{PoP}), Scavenging (J), and Removal Fluxes of ^{210}Po (P) in the Euphotic Zone and Mesopelagic Layer in the Western South China Sea^a

Stn.	Month	Depth (m)	Interval (m)	k		φ		τ_{PoD}	τ_{PoP}	J	P
				(day ⁻¹)		(Year)		(dpm m ⁻² d ⁻¹)			
105A	Aug	775	0–100	0.0024 ± 0.0005	0.025 ± 0.005	1.13 ± 0.22	0.11 ± 0.02	13.3 ± 2.3	17.5 ± 3.7		
			200–700	0.0027 ± 0.0005	0.017 ± 0.003	1.02 ± 0.23	0.16 ± 0.03	53.0 ± 10.4	67.8 ± 16.2		
91	Aug	1756	0–100	0.0021 ± 0.0005	0.022 ± 0.003	1.31 ± 0.28	0.13 ± 0.02	7.0 ± 1.1	11.4 ± 2.0		
			200–1000	0.0003 ± 0.0004	0.024 ± 0.004	9.0 ± 11.2	0.11 ± 0.02	15.4 ± 2.8	120.8 ± 24.4		
102	Aug	4302	0–100	0.0029 ± 0.0005	0.010 ± 0.002	0.95 ± 0.15	0.27 ± 0.05	14.8 ± 2.5	17.0 ± 3.2		
			200–1000	0.0031 ± 0.0004	0.011 ± 0.002	0.90 ± 0.13	0.25 ± 0.05	103.3 ± 16.6	99.1 ± 21.2		
SEATS	Jan	3800	0–100	0.0071 ± 0.0005	0.0065 ± 0.0011	0.39 ± 0.03	0.42 ± 0.07	23.0 ± 1.6	16.8 ± 3.0		
			225–1000	0.0039 ± 0.0003	0.0037 ± 0.0008	0.71 ± 0.05	0.75 ± 0.17	127.8 ± 9.6	66.4 ± 15.0		
	Jul	3800	0–100	0.0055 ± 0.0005	0.026 ± 0.004	0.50 ± 0.04	0.11 ± 0.02	19.4 ± 1.7	19.4 ± 3.4		
			250–1000	0.0019 ± 0.0003	0.0058 ± 0.0016	1.47 ± 0.20	0.47 ± 0.13	74.2 ± 10.4	55.9 ± 15.6		
Oct	3800	0–100	0.0033 ± 0.0002	0.027 ± 0.004	0.84 ± 0.06	0.10 ± 0.01	11.3 ± 0.8	14.1 ± 1.9			
May	3800	200–1000	0.0025 ± 0.0003	0.015 ± 0.005	1.09 ± 0.12	0.18 ± 0.06	96.3 ± 10.6	129.1 ± 40.8			
			0–100	0.0053 ± 0.0003	0.019 ± 0.002	0.51 ± 0.03	0.14 ± 0.01	25.5 ± 1.4	25.5 ± 2.9		
			200–1000	0.0033 ± 0.0002	0.011 ± 0.002	0.82 ± 0.05	0.25 ± 0.05	135.8 ± 7.9	140.6 ± 26.7		

^aData at the SEATS station are calculated from the ^{210}Po - ^{210}Pb data sets [*Wei et al.*, 2014].

plumes. Our results are similar to the observations in the Aleutian Basin, where the ^{210}Po deficiency in mesopelagic and bathypelagic water is ascribed to the enhanced scavenging induced by the laterally transported shelf sediment [Hu *et al.*, 2014]. In fact, a line of evidence in the western SCS, including TPM concentration, particulate ^{210}Po or ^{210}Pb activity, and sinking particle flux (Figures 4 and 5), verified that the ^{210}Po deficiency in mesopelagic water result from shelf resuspended sediment. This cross-shelf transport of sediment and laterally transport of sediment from the top seamount might provide probable interpretations for the ^{210}Po deficiency in some deep water as observed at a few Atlantic GEOTRACES stations [Church *et al.*, 2012; Rigaud *et al.*, 2015].

In this study, the k values of ^{210}Po averaged $0.0020 \pm 0.0015 \text{ day}^{-1}$ in mesopelagic water (Table 2), comparable to $0.0029 \pm 0.0009 \text{ day}^{-1}$ estimated based on the data sets (t test, $p > 0.10$) in the northern SCS [Wei *et al.*, 2014]. The scavenging constant illustrates the intensity of particle-reactive nuclide adsorption on particulate matter in seawater [Yang *et al.*, 2016]. Higher k values correspond to stronger affinity of particle with ^{210}Po . The values in mesopelagic water were close to or slightly lower than those in the euphotic zone (averaging $0.0041 \pm 0.0018 \text{ day}^{-1}$) in the SCS (Table 2) [Yang *et al.*, 2006], indicating a weaker affinity of particle with ^{210}Po in mesopelagic water. Various particulate components have different affinity with ^{210}Po and ^{210}Pb [Yang *et al.*, 2013, 2015b]. It is generally accepted that organic matter usually has stronger affinity for ^{210}Po comparing with ^{210}Pb [Stewart *et al.*, 2007], while inorganic particulate components seem to show little difference in adsorbing them [Nozaki *et al.*, 1997, 1998]. Such a difference is usually quantified by the fractionation factor (i.e., F value) [Guo *et al.*, 2002], defined as the ratio of partition coefficient between two nuclides (i.e., K_d value, calculated by particulate activity divided by dissolved activity and TPM content). In the euphotic zone, particulate matter contains plenty of fresh biogenic organic matter in the SCS [Cai *et al.*, 2008; Yang *et al.*, 2015b], which usually has tight affinity for ^{210}Po [Stewart *et al.*, 2007; Chuang *et al.*, 2014]. After sinking out of the euphotic zone, biogenic particulate organic matter degrades a lot in the upper mesopelagic zone [Yang *et al.*, 2009]. In addition, resuspended sediment contributed largely to the TPM collected in mesopelagic water (Figure 4), probably via the benthic nepheloid layers as observed in the Middle Atlantic Bight (MAB) and the Gulf of Mexico [Santschi *et al.*, 1999; Guo and Santschi, 2000]. Thus, particles in mesopelagic water might be mainly composed of inorganic components, which usually show lower affinity for ^{210}Po than organic matter except for Mn/Fe-(hydr)oxides [Yang *et al.*, 2015a]. The fractionation factor between ^{210}Po and ^{210}Pb (i.e., K_d ratio) also lent supports to this view. As shown in Figure 6, there is a significant linear relation between the fractionation factors and TPM contents in the upper 75 m. If particulate matter is regarded as a mixture of two end-members (i.e., inorganic and organic matter), the fractionation factors would approach one of the end-members following the mixing line when this end-member's contribution increases. Thus, the increase of fractionation factor follows the elevation of TPM indicated that organic matter contribute the majority of particulate matter. Instead, such a relation was not observed for samples below 500 m (Figure 6). The removal constants, revealing the sinking intensity of particulate ^{210}Po , varied from 0.011 to 0.024 day^{-1} with an average of $0.017 \pm 0.007 \text{ day}^{-1}$ in mesopelagic water (Table 2).

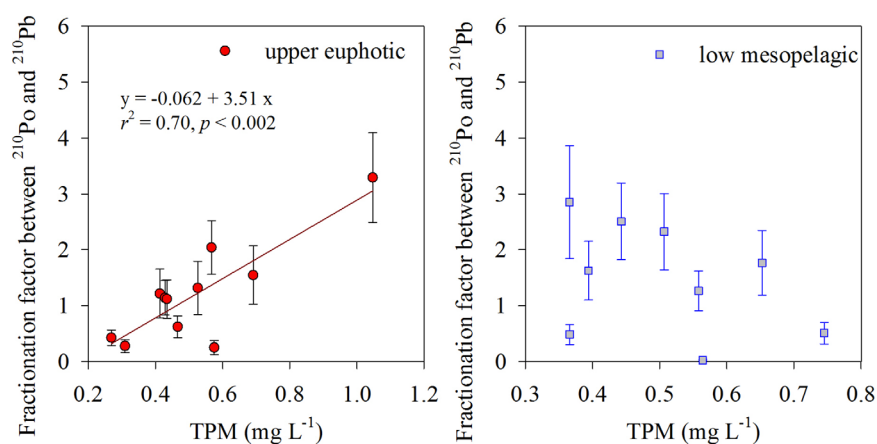


Figure 6. Relations between the fractionation factor (i.e., $K_{d,Po}/K_{d,Pb}$) and TPM concentration in the (left) upper euphotic zone (0–75 m) and (right) low mesopelagic water (500–1000 m).

There is no discernible difference (t test, $p > 0.10$) in the removal constants between mesopelagic and euphotic water (from 0.010 to 0.025 day^{-1}).

The export flux of ^{210}Po out of the mesopelagic layer varied from 67.8 to 120.8 $\text{dpm m}^{-2} \text{d}^{-1}$, averaging $95.9 \pm 26.7 \text{ dpm m}^{-2} \text{d}^{-1}$ (Table 2). Using the data sets of ^{210}Po and ^{210}Pb at station SEATS [Wei *et al.*, 2014], ^{210}Po flux shows a similar range of 55.9–140.6 $\text{dpm m}^{-2} \text{d}^{-1}$ and average of $98.0 \pm 43.0 \text{ dpm m}^{-2} \text{d}^{-1}$ (Table 2). Such comparability probably implied the order of magnitude in terms of ^{210}Po export from the mesopelagic layer in the SCS. Hu *et al.* [2014] reported the ^{210}Po export flux of 412–496 $\text{dpm m}^{-2} \text{d}^{-1}$ out of bathypelagic water in the Aleutian Basin. Together, it appears that the magnitude of ^{210}Po export in various deep oceans has a large variability, indicating a large difference in particle dynamics in the world-wide deep oceans. In comparison with the mesopelagic layer, ^{210}Po showed very lower fluxes out of the euphotic zone, varying from 11.4 to 17.5 $\text{dpm m}^{-2} \text{d}^{-1}$ (avg. $15.3 \pm 3.4 \text{ dpm m}^{-2} \text{d}^{-1}$) at the studied three stations (Figure 1) (t test, $p < 0.01$) and from 14.1 to 25.5 $\text{dpm m}^{-2} \text{d}^{-1}$ (avg. $18.9 \pm 4.9 \text{ dpm m}^{-2} \text{d}^{-1}$) at station SEATS in different seasons (Table 2) (t test, $p < 0.02$). Although particles in mesopelagic water have similar removal constants of ^{210}Po to the euphotic zone as shown by the comparable k values (Table 2), the much higher export fluxes of ^{210}Po indicated that the geochemical cycling of ^{210}Po and other particle-reactive trace elements in mesopelagic water might be a crucial step in understanding trace element cycling on a basin-scale or global scale.

In summary, the lateral transport via benthic nepheloid layer introduced a large amount of resuspended shelf sediment into mesopelagic water in the western SCS. In comparison with biogenic particles in the euphotic zone, resuspended particles include plenty of inorganic components, leading to less fractionation between ^{210}Po and ^{210}Pb . However, ^{210}Po is still preferentially removed relative to ^{210}Pb (Figure 3). Consequently, the benthic nepheloid layers result in a ^{210}Po deficit and short resident times of ^{210}Po in mesopelagic water. Such disequilibrium between ^{210}Po and ^{210}Pb enable the ^{210}Po - ^{210}Pb to track particle dynamics in the benthic nepheloid layer.

4.3. Utilizing of ^{210}Po - ^{210}Pb to Quantify TPM Export Out of the Mesopelagic Layer

Combining all the residence times and removal rates of ^{210}Po , it is clear that particle cycling is very active in the mesopelagic layer in the SCS. Based on the currently limited studies, particulate matter has been found to play important roles in trace elements [Rigaud *et al.*, 2015], nutrients [Kadko *et al.*, 1994] and carbon cycling [Hu *et al.*, 2014; Yang *et al.*, 2016] in deep water with active particle dynamics. Our study provides an opportunity to unravel the particle cycling in mesopelagic water in the SCS. Although the stations are limited, this estimate is a necessary step to try to utilize the ^{210}Po - ^{210}Pb pair to constrain the particle dynamics in mesopelagic water. The TPM export flux was calculated by the inventory of TPM divided by the residence time derived from ^{210}Po - ^{210}Pb disequilibrium [Eppley, 1989]. At the same time, data reported by Wei *et al.* [2014] in the SCS were also reused to calculate the TPM flux out of the mesopelagic layer. The TPM export fluxes were 4.19, 10.20, and 3.61 $\text{g m}^{-2} \text{d}^{-1}$ at stations 105A, 91, and 102, respectively (Figure 7). At station

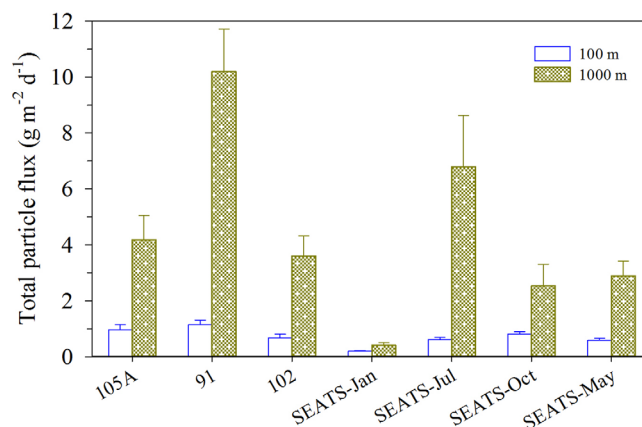


Figure 7. Fluxes of TPM derived from the ^{210}Po - ^{210}Pb approach at the three stations (i.e., 105A, 91, and 102) in the western SCS (this study) and at the SEATS station in the basin [Wei *et al.*, 2014].

SEATS, they varied from 0.41 to 6.80 $\text{g m}^{-2} \text{d}^{-1}$ in terms of different months. For all stations with ^{210}Po deficit in mesopelagic water, the TPM fluxes were, to a varying degree, higher than those out of the euphotic zone (Figure 7), directly supporting the lateral transport of particulate matter to the mesopelagic layer in addition to sinking particle from the euphotic zone. In comparison, the TPM fluxes derived from ^{210}Po were higher than those obtained by sediment traps in the bathypelagic layer in the SCS [Lahajnar *et al.*, 2007; Liu *et al.*, 2014; Schroeder *et al.*, 2015; Dong *et al.*, 2016]. On the one hand, TPM collected in our study includes either suspended particles or

sinking particles. Thus, the fluxes presented here represent the upper limits of particle export out of the mesopelagic layer. On the other hand, sediment trap collected particles in the SCS might have suffered from dissolution, to a varying degree, underestimating the particle fluxes obtained by sediment trap [Sun *et al.*, 2015].

The ^{210}Po - ^{210}Pb pair is widely used to quantify the POC flux out of the euphotic zone [Buesseler *et al.*, 2008; Verdeny *et al.*, 2009; Ceballos-Romero *et al.*, 2016]. This study proved that it could also be used to track the flux of particulate components (such as POC and PON) out of the mesopelagic layer and estimate some crucial parameters (such as residence time) on particulate cycling in mesopelagic water. In addition, the ^{210}Po - ^{210}Pb approach, spatially, allows it to present a high-resolution picture in terms of the mesopelagic particle flux benefiting from their high-resolution sampling. Thus, the ^{210}Po - ^{210}Pb pair could be a powerful tracer for constraining the particle dynamics occurred in mesopelagic water and promote our understanding of the connective roles of mesopelagic particulate in coupling the surface water and bathypelagic processes.

5. Conclusions

A large deficiency of ^{210}Po with respect to ^{210}Pb was observed in mesopelagic water in the western South China Sea, accompanying elevated TPM contents, particulate ^{210}Po and ^{210}Pb . Lateral transport of resuspended sediment from the shelf, probably via benthic nepheloid layer, accounted for the enhanced removal and consequential deficiency of ^{210}Po . The identical residence times of ^{210}Po in both mesopelagic and euphotic zones revealed the very active particle cycling in the mesopelagic layer in the South China Sea. Based on the deficiency of ^{210}Po , the ^{210}Po - ^{210}Pb pair was used to evaluate some crucial processes on particle cycling in mesopelagic water. Given the status that very limited methods are currently available to quantify the particle cycling processes occurred in mesopelagic water, the ^{210}Po - ^{210}Pb technique could provide valuable insights into the residing time scale, degradation and sinking of particulate matter, and facilitate our understanding of particle-reactive trace elements' behavior in mesopelagic water.

Acknowledgments

We thank two anonymous reviewers and Adina Paytan for their insightful comments and suggestions that have contributed to improve this paper. The authors also thank the captain, crew, and scientific party of *R/V SHIYAN3* for their help during sampling. This study was funded jointly by the National Key Research and Development Program of China (2016YFA0601201) and NSFC (41476061 and 41676174). The data supporting the analysis and conclusions can be founded in Tables 1 and 2. The data on SEATS and sediment traps are properly cited and referred to in the reference list.

References

- Bacon, M. P., D. W. Spencer, and P. G. Brewer (1976), $^{210}\text{Pb}/^{226}\text{Ra}$ and $^{210}\text{Po}/^{210}\text{Pb}$ disequilibria in seawater and suspended particulate matter, *Earth Planet. Sci. Lett.*, *32*(2), 277–296.
- Bacon, M. P., R. A. Belostock, M. Tecotzky, K. K. Turekian, and D. W. Spencer (1988), ^{210}Pb and ^{210}Po in ocean water profiles of the continental shelf and slope south of New England, *Cont. Shelf Res.*, *8*, 841–853.
- Buesseler, K. O., C. Lamborg, P. Cai, R. Escoube, R. Johnson, S. Pike, P. Masqué, D. McGillicuddy, and E. Verdeny (2008), Particle fluxes associated with mesoscale eddies in the Sargasso Sea, *Deep Sea Res., Part II*, *55*, 1426–1444.
- Cai, P., W. Chen, M. Dai, Z. Wan, D. Wang, Q. Li, T. Tang, and D. Lv (2008), A high-resolution study of particle export in the southern South China Sea based on ^{234}Th - ^{238}U disequilibrium, *J. Geophys. Res.*, *113*, C04019, doi:10.1029/2007JC004268.
- Cai, P., D. Zhao, L. Wang, B. Huang, and M. Dai (2015), Role of particle stock and phytoplankton community structure in regulating particulate organic carbon export in a large marginal sea, *J. Geophys. Res. Oceans*, *120*, 2063–2095, doi:10.1002/2014JC010432.
- Ceballos-Romero, E., F. A. C. Le Moigne, S. Henson, C. M. Marsay, R. J. Sanders, R. García-Tenorio, and M. V. Milla-Alfageme (2016), Influence of bloom dynamics on particle export efficiency in the North Atlantic: A comparative study of radioanalytical techniques and sediment traps, *Mar. Chem.*, *186*, 198–210.
- Chao, S. Y., P. T. Shaw, and S. Y. Wu (1996), Deep water ventilation in the South China Sea, *Deep Sea Res., Part I*, *43*, 445–466.
- Chen, J., L. Zheng, and M. G. Wiesner (1998), Estimations of primary production and export production in the South China Sea based on sediment trap experiments, *Chin. Sci. Bull.*, *43*, 583–586.
- Chuang, C.-Y., P. H. Santschi, Y.-F. Ho, M. H. Conte, L. Guo, D. Schumann, M. Ayrarov, and Y. H. Li (2013), Role of biopolymers as major carrier phases of Th, Pa, Pb, Po, and Be radionuclides in settling particles from the Atlantic Ocean, *Mar. Chem.*, *157*, 131–143.
- Chuang, C.-Y., P. H. Santschi, Y. Jiang, Y.-F. Ho, A. Quigg, L. Guo, M. Ayrarov, and D. Schumann (2014), Important role of biomolecules from diatoms in the scavenging of particle reactive radionuclides of thorium, protactinium, lead, polonium, and beryllium, in the ocean: A case study with *Phaeodactylum tricornutum*, *Limnol. Oceanogr.*, *59*, 1256–1266.
- Chung, Y., and T. Wu (2005), Large ^{210}Po deficiency in the northern South China Sea, *Cont. Shelf Res.*, *25*(10), 1209–1224.
- Chung, Y., H. C. Chang, and G. W. Hung (2004), Particulate flux and ^{210}Pb determined on the sediment trap and core samples from the northern South China Sea, *Cont. Shelf Res.*, *24*, 673–691.
- Church, T. M., et al. (2012), Intercalibration studies of ^{210}Po and ^{210}Pb in dissolved and particulate seawater samples, *Limnol. Oceanogr. Methods*, *10*(10), 776–789.
- Cochran, J. K., M. P. Bacon, S. Krishnaswami, and K. K. Turekian (1983), ^{210}Po and ^{210}Pb distributions in the central and eastern Indian Ocean, *Earth Planet. Sci. Lett.*, *65*(2), 433–452.
- Dong, Y., Q. P. Li, Z. Wu, and J. Zhang (2016), Variability in sinking fluxes and composition of particle-bound phosphorus in the Xisha area of the northern South China Sea, *Deep Sea Res., Part I*, *118*, 1–9.
- Eppley, R. W. (1989), New production: History, methods, problems, in *Productivity of The Ocean: Present and Past*, edited by W. H. Berger, V. S. Smetacek, and G. Wefer, pp. 85–97, John Wiley, New York.
- Estapa, E. L., J. A. Breier, and C. R. German (2015), Particle dynamics in the rising plume at Piccard Hydrothermal Field, Mid-Cayman Rise, *Geochem. Geophys. Geosyst.*, *16*, 2762–2774, doi:10.1002/2015GC005831.

- Friedrich, J., and M. M. Rutgers van der Loeff (2002), A two-tracer (^{210}Po - ^{234}Th) approach to distinguish organic carbon and biogenic silica export flux in the Antarctic Circumpolar Current, *Deep Sea Res., Part I*, 49(1), 101–120.
- Gaye, B., M. G. Wiesner, and N. Lahajnar (2009), Nitrogen sources in the South China Sea, as discerned from stable nitrogen isotopic ratios in rivers, sinking particles, and sediments, *Mar. Chem.*, 114, 72–85.
- Guo, L., and P. H. Santschi (2000), Sedimentary sources of old high molecular weight dissolved organic carbon from the ocean margin benthic nepheloid layer, *Geochim. Cosmochim. Acta*, 64, 651–660.
- Guo, L., M. Chen, and C. Gueguen (2002), Control of Pa/Th ratio by particulate chemical composition in the ocean, *Geophys. Res. Lett.*, 29(20), 1961, doi:10.1029/2002GL015666.
- Hong, G., M. Baskaran, T. M. Church, and M. Conte (2013), Scavenging, cycling and removal fluxes of ^{210}Po and ^{210}Pb at the Bermuda time-series study site, *Deep Sea Res., Part II*, 93, 108–118.
- Hu, W., M. Chen, W. Yang, R. Zhang, Y. Qiu, and M. Zheng (2014), Enhanced particle scavenging in deep water of the Aleutian Basin revealed by ^{210}Po - ^{210}Pb disequilibria, *J. Geophys. Res. Oceans*, 119, 3235–3248, doi:10.1002/2014JC009819.
- Kadko, D., M. P. Bacon, and A. Hudson (1987), Enhanced scavenging of ^{210}Pb and ^{210}Po by processes associated with the East Pacific Rise near $8^{\circ}45'\text{N}$, *Earth Planet. Sci. Lett.*, 81(4), 349–357.
- Kadko, D., R. Feely, and G. Massoth (1994), Scavenging of ^{234}Th and phosphorus removal from the hydrothermal effluent plume over the North Cleft segment of the Juan de Fuca Ridge, *J. Geophys. Res.*, 99, 5017–5024.
- Kara, A. B., P. A. Rochford, and H. E. Hurlburt (2000), An optimal definition for ocean mixed layer depth, *J. Geophys. Res.*, 105, 16,803–16,821.
- Kim, G. (2001), Large deficiency of polonium in the oligotrophic ocean's interior, *Earth Planet. Sci. Lett.*, 192, 15–21.
- Lahajnar, N., M. G. Wiesner, and B. Gaye (2007), Fluxes of amino acids and hexosamines to the deep South China Sea, *Deep Sea Res., Part I*, 54, 2120–2144.
- Li, F., L. Li, X. Wang, and C. Liu (2002), Water masses in the South China Sea and water exchange the Pacific and the South China Sea, *J. Ocean Univ. Qingdao*, 1, 19–24.
- Liu, J., R. Xiang, Z. Chen, M. Chen, W. Yan, L. Zhang, and H. Chen (2013), Sources, transport and deposition of surface sediments from the South China Sea, *Deep Sea Res., Part I*, 71, 92–102.
- Liu, J., P. D. Clift, W. Yan, Z. Chen, H. Chen, R. Xiang, and D. Wang (2014), Modern transport and deposition of settling particles in the northern South China Sea: Sediment trap evidence adjacent to Xisha Trough, *Deep Sea Res., Part I*, 93, 145–155.
- Liu, Z., et al. (2016), Source-to-sink transport processes of fluvial sediments in the South China Sea, *Earth Sci. Rev.*, 153, 238–273.
- Maiti, K., S. Bosu, E. J. D'Sa, P. L. Adhikari, M. Sutor, and K. Longnecker (2016), Export fluxes in northern Gulf of Mexico—Comparative evaluation of direct, indirect and satellite-based estimates, *Mar. Chem.*, 184, 60–77.
- Murray, J. W., B. Paul, J. P. Dunne, and T. Chapin (2005), ^{234}Th , ^{210}Pb , ^{210}Po and stable Pb in the central equatorial Pacific: Tracers for particle cycling, *Deep Sea Res., Part I*, 52(11), 2109–2139.
- Nozaki, Y., and S. Tsunogai (1976), ^{226}Ra , ^{210}Pb and ^{210}Po disequilibria in the Western North Pacific, *Earth Planet. Sci. Lett.*, 32(2), 313–321.
- Nozaki, Y., J. Zhang, and A. Takeda (1997), ^{210}Pb and ^{210}Po in the equatorial Pacific and the Bering Sea: The effects of biological productivity and boundary scavenging, *Deep Sea Res., Part II*, 44(9), 2203–2220.
- Nozaki, Y., F. Dobashi, Y. Kato, and Y. Yamamoto (1998), Distribution of Ra isotopes and the ^{210}Pb and ^{210}Po balance in surface seawaters of the mid Northern Hemisphere, *Deep Sea Res., Part I*, 45, 1263–1284.
- Rigaud, S., V. Puigcorbe, P. Camarero, N. Casacuberta, M. Rocamarti, J. Garciaorellana, C. R. Beniteznelson, P. Masque, and T. M. Chuech (2013), A methods assessment and recommendations for improving calculations and reducing uncertainties in the determination of ^{210}Po and ^{210}Pb activities in seawater, *Limnol. Oceanogr. Methods*, 11(10), 561–571.
- Rigaud, S., G. Stewart, M. Baskaran, D. Marsan, and T. Church (2015), ^{210}Po and ^{210}Pb distribution, dissolved-particulate exchange rates, and particulate export along the North Atlantic US GEOTRACES GA03 section, *Deep Sea Res., Part II*, 116, 60–78.
- Roca-Martí, M., V. Puigcorbe, M. M. Rutgers van der Loeff, C. Katlein, M. Fernandezmendez, I. Peeken, and P. Masque (2016), Carbon export fluxes and export efficiency in the central Arctic during the record sea-ice minimum in 2012: A joint ^{234}Th / ^{238}U and ^{210}Po / ^{210}Pb study, *J. Geophys. Res.*, 121, 5030–5049, doi:10.1002/2016JC011816.
- Santschi, P. H., L. Guo, I. D. Walsh, M. S. Quigley, and M. Baskaran (1999), Boundary exchange and scavenging of radionuclides in continental margin waters of the Middle Atlantic Bight: Implications for organic carbon fluxes, *Cont. Shelf Res.*, 19, 609–636.
- Schroeder, A., M. G. Wiesner, and Z. Liu (2015), Fluxes of clay minerals in the South China Sea, *Earth Planet. Sci. Lett.*, 430, 30–42.
- Shaw, P. T., and S. Y. Chao (1994), Surface circulation in the South China Sea, *Deep Sea Res., Part I*, 41, 1663–1683.
- Siegel, D. A., E. Fields, and K. O. Buesseler (2008), A bottom-up view of the biological pump: Modeling source funnels above ocean sediment traps, *Deep Sea Res., Part I*, 55, 108–127.
- Stewart, G., J. K. Cochran, J. Xue, C. Lee, S. G. Wakeham, R. A. Armstrong, P. Masqué, and J. C. Miquel (2007), Exploring the connection between ^{210}Po and organic matter in the northern Mediterranean, *Deep Sea Res., Part I*, 54, 415–427.
- Stewart, G. M., S. B. Moran, and M. W. Lomas (2010), Seasonal POC fluxes at BATS estimated from ^{210}Po deficits, *Deep Sea Res., Part I*, 57(1), 113–124.
- Su, K., J. Du, M. Baskaran, and J. Zhang (2017), ^{210}Po and ^{210}Pb disequilibrium at the PN section in the East China Sea, *J. Environ. Radioact.*, doi:10.1016/j.jenvrad.2016.07.031.
- Sun, L., H. Li, J. Tim, L. Ran, H. Jin, J. Zhang, W. Martin, and J. Chen (2015), Underestimation of C and N flux in the northern South China Sea due to dissolution in sediment trap samples [in Chinese with English abstract], *Acta Oceanol. Sin.*, 37, 19–26.
- Turekian, K. K., and Y. Nozaki (1980), ^{210}Po and ^{210}Pb in the Eastern South Pacific—the role of upwelling on their distributions in the water column, in *Isotope Marine Chemistry*, edited by E. D. Goldberg, Y. Horibe, and K. Saruhashi, pp. 157–164, Uchida Rokkakuho, Tokyo.
- Verdeny, E., P. Masqué, J. Garcia-Orellana, C. Hanfland, J. K. Cochran, and G. M. Stewart (2009), POC export from ocean surface waters by means of ^{234}Th / ^{238}U and ^{210}Po / ^{210}Pb disequilibria: A review of the use two radiotracer pairs, *Deep Sea Res., Part II*, 56, 1502–1518.
- Wang, H., Q. Yang, F. Ji, M. D. Lilley, and H. Zhou (2012), The geochemical characteristics and Fe(II) oxidation kinetics of hydrothermal plumes at the Southwest Indian Ridge, *Mar. Chem.*, 134–135, 29–35.
- Wang, P., Q. Li, and J. Tian (2014), Pleistocene paleoceanography of the South China Sea: Progress over the last 20 years, *Mar. Geol.*, 352, 381–396.
- Wei, C., S. Y. Lin, D. D. Sheu, W. Chou, M. C. Yi, P. H. Santschi, and L. Wen (2011), Particle-reactive radionuclides (^{234}Th , ^{210}Pb , ^{210}Po) as tracers for the estimation of export production in the South China Sea, *Biogeosciences*, 8(12), 3793–3808.
- Wei, C., M. C. Yi, S. Y. Lin, L. Wen, and W. H. Lee (2014), Seasonal distributions and fluxes of ^{210}Pb and ^{210}Po in the northern South China Sea, *Biogeosciences*, 11(23), 6813–6826.
- Wei, C., C. Chia, W. Chou, and W. Lee (2017), Sinking fluxes of ^{210}Pb and ^{210}Po in the deep basin of the northern South China Sea, *J. Environ. Radioact.*, doi:10.1016/j.jenvrad.2016.05.026.

- Yang, W., Y. Huang, M. Chen, L. Zhang, H. Li, G. Liu, and Y. Qiu (2006), Disequilibria between ^{210}Po and ^{210}Pb in surface waters of the southern South China Sea and their implications, *Sci. China Ser. D*, *49*(1), 103–112.
- Yang, W., Y. Huang, M. Chen, Y. Qiu, A. Peng, and Z. Lei (2009), Export and remineralization of POM in the Southern Ocean and the South China Sea estimated from $^{210}\text{Po}/^{210}\text{Pb}$ disequilibria, *Chin. Sci. Bull.*, *54*, 2118–2123.
- Yang, W., Y. Huang, M. Chen, Y. Qiu, H. Li, and L. Zhang (2011), Carbon and nitrogen cycling in the Zhubi coral reef lagoon of the South China Sea as revealed by ^{210}Po and ^{210}Pb , *Mar. Pollut. Bull.*, *62*(5), 905–911.
- Yang, W., L. Guo, C. Y. Chuang, D. Schumann, M. Ayrarov, and P. H. Santschi (2013), Adsorption characteristics of ^{210}Pb , ^{210}Po and ^7Be onto micro-particle surfaces and the effects of macromolecular organic compounds, *Geochim. Cosmochim. Acta*, *107*, 47–64.
- Yang, W., L. Guo, C. Y. Chuang, P. H. Santschi, D. Schumann, and M. Ayrarov (2015a), Influence of organic matter on the adsorption of ^{210}Pb , ^{210}Po and ^7Be and their fractionation on nanoparticles in seawater, *Earth Planet. Sci. Lett.*, *423*, 193–201.
- Yang, W., et al. (2015b), Influence of a decaying cyclonic eddy on biogenic silica and particulate organic carbon in the tropical South China Sea based on ^{234}Th - ^{238}U disequilibrium, *PLoS ONE*, *10*(8), e0136948, doi:10.1371/journal.pone.0136948.
- Yang, W., X. Zhang, M. Chen, and Y. Qiu (2016), Unusually low ^{234}Th in a hydrothermal effluent plume over the Southwest Indian Ridge, *Geochem. Geophys. Geosyst.*, *17*, 3815–3824, doi:10.1002/2016GC006580.
- Zhang, X., J. Chen, L. Xiang, J. Fang, D. Li, Y. Zhu, Y. Ou, and Y. Fan (2014), A preliminary study on the characteristics of marine nepheloid layers in the northern South China Sea and their influential factors [in Chinese with English abstract], *Acta Oceanol. Sin.*, *36*, 51–65.